NAVAL POSTGRADUATE SCHOOL

MONTEREY, CALIFORNIA

THESIS

GAME-THEORETIC MODELS FOR RAPID OPERATIONAL AIRLIFT NETWORK DESIGN IN CONTESTED ENVIRONMENTS

by

Alexander J. Cooper

March 2023

Thesis Advisor: Jefferson Huang
Second Reader: Peter A. Nesbitt

THIS PAGE INTENTIONALLY LEFT BLANK

REPORT DOCUMENTATION PAGE	*Form Approved OMB No. 0704-0188*

1. AGENCY USE ONLY ***(Leave blank)***	**2. REPORT DATE** March 2023	**3. REPORT TYPE AND DATES COVERED** Master's thesis

4. TITLE AND SUBTITLE
GAME-THEORETIC MODELS FOR RAPID OPERATIONAL AIRLIFT NETWORK DESIGN IN CONTESTED ENVIRONMENTS

5. FUNDING NUMBERS

6. AUTHOR(S) Alexander J. Cooper

7. PERFORMING ORGANIZATION NAME(S) AND ADDRESS(ES)
Naval Postgraduate School
Monterey, CA 93943-5000

8. PERFORMING ORGANIZATION REPORT NUMBER

9. SPONSORING / MONITORING AGENCY NAME(S) AND ADDRESS(ES)
N/A

10. SPONSORING / MONITORING AGENCY REPORT NUMBER

11. SUPPLEMENTARY NOTES The views expressed in this thesis are those of the author and do not reflect the official policy or position of the Department of Defense or the U.S. Government.

12a. DISTRIBUTION / AVAILABILITY STATEMENT Approved for public release. Distribution is unlimited.	**12b. DISTRIBUTION CODE** A

13. ABSTRACT (maximum 200 words)

The growing threat of conflict with near-peer adversaries requires a robust air-routing plan to transport personnel and cargo effectively. In developing these plans, the U.S. Air Force's Air Mobility Command (AMC) must account for the dynamic nature of inter-theater operations in a contested environment. Currently, AMC planners predominantly calculate resource allocations manually, which contributes to slower plan implementation and potentially suboptimal solutions. Starting with a proven AMC model, which provides an optimal use of aircraft, cargo allocation, and airfields, we add model features that help determine how to attack this airlift network, optimally delaying the delivery of cargo to operationally relevant locations. The results identify vulnerabilities and provide AMC planners with a prescription of airfield resource allocation that maximizes the movement of cargo. This model delivers a quantitative assessment of an adversary's (whether weather or competitor) ability to delay the mission that can be used to guide policymakers in providing a robust air mobility capability.

14. SUBJECT TERMS
game theory, attacker-defender, Air Mobility Command, AMC, inter-theater

15. NUMBER OF PAGES 63

16. PRICE CODE

17. SECURITY CLASSIFICATION OF REPORT	**18. SECURITY CLASSIFICATION OF THIS PAGE**	**19. SECURITY CLASSIFICATION OF ABSTRACT**	**20. LIMITATION OF ABSTRACT**
Unclassified	Unclassified	Unclassified	UU

NSN 7540-01-280-5500 Standard Form 298 (Rev. 2-89) Prescribed by ANSI Std. 239-18

THIS PAGE INTENTIONALLY LEFT BLANK

Approved for public release. Distribution is unlimited.

GAME-THEORETIC MODELS FOR RAPID OPERATIONAL AIRLIFT NETWORK DESIGN IN CONTESTED ENVIRONMENTS

Alexander J. Cooper
Lieutenant Commander, United States Navy
BS, Lander College, 2011

Submitted in partial fulfillment of the
requirements for the degree of

MASTER OF SCIENCE IN OPERATIONS RESEARCH

from the

NAVAL POSTGRADUATE SCHOOL
March 2023

Approved by: Jefferson Huang
Advisor

Peter A. Nesbitt
Second Reader

W. Matthew Carlyle
Chair, Department of Operations Research

THIS PAGE INTENTIONALLY LEFT BLANK

ABSTRACT

The growing threat of conflict with near-peer adversaries requires a robust air-routing plan to transport personnel and cargo effectively. In developing these plans, the U.S. Air Force's Air Mobility Command (AMC) must account for the dynamic nature of inter-theater operations in a contested environment. Currently, AMC planners predominantly calculate resource allocations manually, which contributes to slower plan implementation and potentially suboptimal solutions. Starting with a proven AMC model, which provides an optimal use of aircraft, cargo allocation, and airfields, we add model features that help determine how to attack this airlift network, optimally delaying the delivery of cargo to operationally relevant locations. The results identify vulnerabilities and provide AMC planners with a prescription of airfield resource allocation that maximizes the movement of cargo. This model delivers a quantitative assessment of an adversary's (whether weather or competitor) ability to delay the mission that can be used to guide policymakers in providing a robust air mobility capability.

THIS PAGE INTENTIONALLY LEFT BLANK

Table of Contents

List of Figures

THIS PAGE INTENTIONALLY LEFT BLANK

List of Tables

THIS PAGE INTENTIONALLY LEFT BLANK

List of Acronyms and Abbreviations

AFB	Air Force Base
AFOSR	Air Force Office of Scientific Research
AMC	Air Mobility Command
AOP	Airlift Optimization Planning Tool
COCOM	Combatant Command
DOD	Department of Defense
ICAO	International Civil Aviation Organization
ILP	Integer Linear Program
MOG	Maximum (aircraft) on Ground
NM	Nautical Miles
NPS	Naval Postgraduate School
PMOG	Parking Maximum on Ground
PRC	People's Republic of China
RANG	Research and Development Corporation
RODAN	Rapid Operational Design of Airlift Networks
USAF	United States Air Force
USTRANSCOM	United States Transportation Command
WMOG	Working Maximum on Ground

THIS PAGE INTENTIONALLY LEFT BLANK

Executive Summary

The increasing risk of conflict with near-peer adversaries has shifted the mindset of the Department of Defense from operating in a largely uncontested logistics environment to a contested one. A key component in military logistical superiority is the global air mobility that is currently provided by the United States Air Force's (USAF) Air Mobility Command (AMC). To support and sustain strategic, operational, and tactical levels of war efforts, AMC has identified the need to rapidly design and evaluate its airlift networks. AMC is consolidating its emerging decision-enabling tools under its newly developed Rapid Operational Design of Airlift Networks (RODAN) project, which is sponsored and championed by the Air Force Office of Scientific Research (AFOSR).

Key considerations for developing and evaluating airlift networks include airfield ramp space, ground service equipment, personnel, and the limitations of personnel. Working Maximum aircraft on Ground (WMOG) is a commonly used measure of airfield capacity that represents the amount of equipment and personnel required to process a certain number of aircraft efficiently and safely at an airfield. The finite amount of WMOG available and the dynamic nature of airlift requirements pose an exceptionally difficult challenge for AMC planners. Ineffective allocation of WMOG across AMC's network of airfields can lead to delivery delays, safety hazards, and failure of mission requirements. Though difficult in an uncontested setting, a contested environment will augment these challenges and exacerbate shortcomings.

This thesis contributes to RODAN by modeling the WMOG allocation problem in a contested environment as an attacker-defender model. The model is a two-player zero-sum game that can indicate which airfields are most valuable to attack based on AMC's allocation of WMOG, and prescribes to AMC how to shift its WMOG given the possibility of such an attack. We call this model the Attacker-Defender Airlift Planning Tool (ADAPT). From the attacker's perspective, the goal is to attack AMC's network in a way that minimizes the flow of cargo through its network of airfields. Based on the attacker's attack allocation, the defender's goal is to move WMOG within the network of airfields that will maximize the movement of cargo. The opposing objectives reveal airlift network vulnerabilities to AMC planners, and also provide AMC planners with a general plan that leverages the resources within its current network.

ADAPT enables quick airlift network vulnerability detection by providing a means of modeling possible threats. After inputting their WMOG allocation to their various airfields and cargo movement requirement, AMC planners can discuss the impacts of various threats to their airfields and input this impact into ADAPT. An attack as severe as the complete removal of airfield capability or as routine as weather delays can impact the flow of cargo. An added benefit of ADAPT is that it can show AMC planners how resilient their current network is against potential worst-case disruptions. ADAPT provides significant complementary contributions to existing tools within AMC's RODAN initiative.

We first illustrate the model using a simple network with five airfields, where one airfield supplies the cargo, one airfield demands cargo, and where the remaining trans-shipment airfields may be attacked. For this network, ADAPT can be solved on a Macbook Pro M1 (2021) in less than one second. Then, we consider a larger scenario that requires the movement of 2000 cargo-tons of cargo, and involves 55 WMOG units allocated across 24 airfields within the U.S. Indo-Pacific Command area of responsibility. We use this scenario to illustrate how to interpret ADAPT's outputs. These include the worst-case airfields to attack, as well as the percentage of cargo moved after an attack. We explored the impact of up to 10 attacks, each of which had an average computation time of less than five seconds. For this scenario, we found that the allocation of WMOG was still able to move 100% of cargo through the network for up to two attacks. Unsurprisingly, as the number of attacks increased, the percentage of cargo movement through the network decreased.

As AMC develops decision support tools, it must consider the adversary's actions when planning its airlift networks. ADAPT aids AMC planners by detecting vulnerabilities in their network that can be exploited by adversaries. Additionally, ADAPT lays the foundation for incorporating the impact of an attack to airlift plans and infuses contested environments into AMC planner conversations. Identifying which airfields are most valuable for an attacker to attack and having an idea of the overall impact of the attack will assist planners in developing alternative airlift networks to accomplish mission objectives.

Acknowledgments

First, I would like to thank my advisor, Dr. Jefferson Huang, and second reader, LTC Pete Nesbitt. I appreciate your support and flexibility throughout my thesis journey. I would not have been able to achieve this critical milestone without you. I would also like to thank Dr. Bradford Davis for providing his insightful perspective on my thesis. To my mom, Cecilia Cooper, and siblings, Raymond, Eryan, and Renee, thank you for your encouragement. I am so thankful that we have remained close despite living so far apart. Finally, I would like to thank my beautiful wife, Sara Beth, for her love and support. Throughout our time together, you have been a constant source of strength, growth, calm, and joy. I look forward to the many adventures we have ahead of us.

THIS PAGE INTENTIONALLY LEFT BLANK

CHAPTER 1:
Introduction

The 2022 National Defense Strategy (NDS), Department of Defense (2022), identifies the emergence of the People's Republic of China (PRC) as a pacing challenge that is capable of disrupting our currently uncontested logistics. This recognition has prompted a response by senior military leaders to prepare for potential conflicts with near-peer adversaries in contested environments. It is critical that Air Mobility Command (AMC) be fully aligned with the NDS since its mission is to be a key enabler of warfighting capabilities. To build an enduring advantage, AMC planners must be able to rapidly design, refine, and operate a global air mobility plan with quantifiable means to best support Air Force leadership, joint strategy, and approved military plans. Finite resources, time, and adversarial influence can cause vast logistical challenges that stress the need to equip our AMC planning team with tools that enhance their capabilities and streamline analysis. This thesis proposes a model that identifies vulnerabilities in AMC's existing network of airfields and prescribes resource adjustments within its network. To better understand how this tool can be useful, it is important to understand details about AMC's overall mission and contribution to the Department of Defense (DOD).

1.1 Air Mobility Command

AMC's mission is to expeditiously move cargo and personnel in support of strategic, operational, and tactical requirements. Air Mobility Command (2023a) states that it is comprised of approximately 110,000 personnel and operates the C-5 Galaxy, KC-10 Extender, C-17 Globemaster III, C-130 Hercules, C-130J Super Hercules, KC-46 Pegasus, and KC-135 Stratotanker. Additionally, Air Mobility Command (2023a) states the operational support aircraft operated by AMC are the VC-25 (Air Force 1), C-20, C-21, C-32, and C-40. Table 1.1 shows the specific mission sets and capabilities of the main types of aircraft that Air Mobility Command (2023b) operates.

Table 1.1. AMC Aircraft Mission and Capabilities. Adapted from Air Mobility Command (2023b)

Aircraft Type	Mission Set	Capabilities
C-130 Hercules	Tactical Airlift Missions	Can operate from rough, dirt strips. Primary transport for airdropping troops and equipment into hostile areas.
C-17 Globemaster III	Flexible/Multi-Mission	Most flexible cargo aircraft. Rapid strategic delivery of troops and cargo. Can deliver to main operating bases or to forward deployed areas.
C-21	Passenger and Cargo	Military version of Learjet 35A business jet.
C-32	VIP Transportation	Safe, comfortable, and reliable transportation of U.S. leaders. Transport the Vice President, First Lady, Cabinet members, and Congress members.
C-37 A/B	VIP Transportation	Safe reliable movement of high-ranking government officials.
C-40 B/C	VIP Transportation	Safe reliable movement of Cabinet members and Congress members.
C-5 A/B/C Galaxy	Strategic Transportation	Largest aircraft in U.S. Air Force inventory. Primary mission is to transport cargo and personnel.
Civil Reserve Air Fleet	Augmenting Forces	Augment airlift capabilities when needed.

1.2 Maximum on Ground

To aid in the planning process, AMC uses various aggregate values known as maximum on ground (MOG). MOG provides AMC planners with a common unit to aid in airlift network planning (Whitlow 2022). There are various applications of MOG such as passenger MOG (paxMOG), parking MOG (PMOG), or maintenance MOG (mxMOG) (Secretary of the Air

Force 2018). These MOGs are different restrictions on the capabilities of an airfield and are determined through subject matter expertise discussion (Whitlow 2022). The primary value associated with this thesis is Working Maximum on Ground (WMOG). According to Secretary of the Air Force (2018), WMOG is an aggregate of the equipment and personnel required to process an aircraft through an airfield. In the context of this thesis, WMOG enables the flow of cargo through AMC's network of airfields and derive flow of cargo capabilities as defined and overseen by the Secretary of the Air Force (2018).

1.3 Rapid Operational Design of Airlift Networks

This thesis is in support of Rapid Operational Design of Airlift Networks (RODAN), which is a current US Air Force initiative sponsored by the Air Force Office of Scientific Research. RODAN consists of a suite of applications intended to enable rapid airlift design and evaluation. The model developed in this thesis builds on the Airlift Optimization Planning Tool (AOPT), which was developed by Whitlow (2022) in support of RODAN. According to Whitlow (2022) AOPT has provided AMC planners with a useful decision aid that prescribes WMOG allocation over a planning horizon of 30 days. It accounts for various airfield constraints, such as airfield capacities and available aircraft at each airfield. Although it provides AMC planners with a useful output of WMOG allocation, it does not account for actions that an adversary may take to obstruct airlift capabilities.

This thesis is organized as follows. Chapter 2 presents a literature review on airlift problems, attacker-defender formulation and solution algorithm, as well as discussion on key USAF technical documentation. Chapter 3 provides in-depth information about the model developed and the Benders decomposition algorithm used to solve it. Chapter 4 analyzes the output of the model by applying it to two notional networks. Chapter 5 provides conclusions about the thesis, disseminates recommendations on how to use the model, and proposes future work. The appendix consolidates all findings from the outputs generated by the model in Chapter 4.

THIS PAGE INTENTIONALLY LEFT BLANK

CHAPTER 2:
Literature Review

The purpose of this chapter is to review prior research that is utilized in this thesis. We review prior work on airlift optimization, interdiction models, and United States Air Force literature.

2.1 Airlift Optimization

This work conducted by Brown et al. (2013) was critical in supporting intra-theater military operations in Iraq and Afghanistan. Brown et al. (2013) develop an integer linear programming model that plans routes that maximize the amount of cargo movement. This thesis draws a lot of inspiration from the goal of ATEM. ATEM is constrained by similar things as aircraft availability and capacity, as well as ramp capacity. This thesis deviates from the ATEM model by exploring inter-theater military airlift operations. Intra-theater is the movement of cargo and personnel through a smaller geographic region. Inter-theater is the movement of cargo and personnel through various global regions.

Whitlow (2022) develops an integer linear program called Airlift Optimization Planning Tool (AOPT) to support AMC's RODAN initiative. The model has an objective function that minimizes risk to mission and minimizes risk to force. The model is constrained by aircraft and airfield limitations, while incorporating data provided by AMC planners. He utilizes AOPT to solve a 30 day scenario with various supply and demand inputs. The model ultimately prescribes daily WMOG movement and aircraft assignment that satisfies a user's supply and demand input.

2.2 Interdiction Models

Alderson et al. (2011) describes and formulates a defender-attacker-defender (DAD) model and provides an algorithm which solves it. They demonstrate the DAD model by applying it to a small transportation related scenario. The defender initially chooses from a selection of infrastructure investment decisions, the attacker observes the investments then attacks the defender's infrastructure, and the defender finally chooses a network operation plan that minimizes costs. Alderson et al. (2011) concludes their research by sharing their empirical results and providing insights for future applications.

Cormican et al. (1998) describes, formulates, and solves a stochastic version of a network interdiction problem. The objective of the described network is to maximize flow. The purpose of exploring a stochastic network interdiction was to apply it to military-related challenges. They then apply their stochastic network interdiction model to a network consisting of over 100 nodes, 180 arcs, and 80 arcs susceptible to attack. They then use Benders decomposition to solve their model.

Trask (2022) presents two attacker-defender model structures and techniques to calculate an optimal solution. The attacker-defender models he describes are shortest path interdiction and minimizing maximum flow. He solves both models by using Benders decomposition and a dual integer linear program. After describing the solving techniques in detail, he provides empirical data on the computational time of finding an optimal solution as the number of nodes in the network increases. This thesis leverages the basic design of the min-max flow described in Trask (2022) thesis and solves using Benders decomposition. More details on the structure and solution technique will be described in Chapter 3.

2.3 United States Air Force Literature

Secretary of the Air Force (2018) is provided to AMC planners to aid in war and peacetime air mobility efforts. It contains valuable information the aids in AMC planner calculation and decision-making. It contains four basic parts: formulas for airlift/air refueling/aeromedical evacuation, example calculations, tables containing heuristics for calculation purposes, and terms and definitions. The information provided in the pamphlet offer a big picture perspective on airlift planning efforts. For this thesis, we leveraged cargo processing numbers which aid in computing maximum flow through our network.

CHAPTER 3: Methodology

In this chapter, we formulate an attacker-defender model of WMOG allocation in a contested environment, called ADAPT (Attacker-Defender Airlift Planning Tool). The chapter starts by describing the sets, parameters, and decision variables for the model. The formulation of the model is provided in standard NPS form, followed by a detailed description of the objective function and constraints. The description of the decomposition algorithm we use to solve the attacker-defender model is found toward the end of the chapter.

3.1 ADAPT Model

AMC is the operator of an air mobility network seeking to adjust the disposition of WMOG across available airfields in order to maximize the flow of cargo through the overall network. We henceforth use the term of *attacker* as an entity (e.g., nation, group of nations, non-state actors) trying to minimize the flow of cargo through AMC's network of airfields. The attacker seeks to reduce the flow of cargo through a limited number airfields through conventional or unconventional means. The specific means of attack modelled informs the maximum number of attacks and effect of the attack measured by reduced effectiveness of WMOG at the attacked airfield. AMC is the *defender* of the network, actively adjusting the placement of the WMOG to reduce the effectiveness of the attacks and maximize overall cargo flow.

We formulate a model to attack AMC's transportation network of airfields. This attacker-defender model, named ADAPT, identifies optimal attacks, subject to means of attack constraints, while a defender of the network observes any attacks and moves WMOG and allocates aircraft in order to limit the effects of the set of airfields attacked. ADAPT can represent a single means of attack and how it affects the overall cargo flow. It can capture various impacts of an attack based on inputs provided by AMC planners. ADAPT can be used to detect airlift network vulnerabilities, prescribe WMOG movement between airfields, and prescribe aircraft needed to move cargo requirements.

Index Sets

$\mathcal{N}$	set of airfields
$\mathcal{A}$	set of flight legs

Parameter Definitions

$maxmog_i$	Available WMOG if at location i. [WMOG]
$maxmogmoved_i$	Limit of WMOG that can be moved out of airfield i. [WMOG]
$mogremoved_i$	Number of WMOG removed at airfield i if airfield i is attacked. [Integer]
$cargocap$	Amount of cargo that can be moved by an aircraft. [cargo-tons]
$startmog_i$	Initial amount of WMOG allocated to airfield i. [WMOG]
$mogused_i$	WMOG used by each aircraft at airfield i. [WMOG]
$supply$	Amount of cargo that needs to be moved throughout network. [cargo-tons]
s	Node that aggregates supply airfields. [airfield]
t	Node that aggregates demand airfields. [airfield]
$maxattack$	Maximum attacks the attacker can allocate [attacks]
q_i	Penalty for flow through airfield i, if it is attacked

Variables

X_{ij}	Cargo flow from airfield i to airfield j. [cargo-tons, WMOG processing capability]
X_{ts}	Total cargo flow for entire network. [cargo-tons, WMOG processing capability]
A_{ij}	Total number of aircraft assigned to move cargo from airfield i to airfield j. [Number of Aircraft]
M_{ij}	WMOG units moved from airfield i to airfield j. [WMOG Units]
Y_i	$\begin{cases} 1, \text{ if airfield } i \text{ is selected for attack} \\ 0, \quad \text{otherwise} \end{cases}$

ADAPT Formulation

$$\min_{Y} \max_{X,A,M} \quad X_{ts} - \sum_{i \in \mathcal{N}} q_i Y_i \left[\sum_{j:(i,j)\in\mathcal{A}} X_{ij} + \sum_{j:(j,i)\in\mathcal{A}} X_{ji} \right] \tag{3.1}$$

$$\text{subject to} \quad \sum_{j:(i,j)\in\mathcal{A}} X_{ij} - \sum_{j:(j,i)\in\mathcal{A}} X_{ji} = \begin{cases} X_{ts}, & \text{if } i = s \\ 0, & \text{if } i \notin \mathcal{N} \setminus \{s,t\} \\ -X_{ts} & \text{if } i = t \end{cases} \tag{3.2}$$

$$X_{ij} \leq \begin{cases} cargocap \cdot A_{ij} & \text{if } (i,j) \in \mathcal{A} \\ supply & \text{if } (i,j) = (t,s) \end{cases} \tag{3.3}$$

$$\sum_{(i,j)\in\mathcal{A}} M_{ij} \leq maxmogmoved \tag{3.4}$$

$$- \sum_{j:(i,j)\in\mathcal{A}} M_{ij} + \sum_{j:(j,i)\in\mathcal{A}} M_{ji} \leq maxmog_i - startmog_i \qquad \forall i \in \mathcal{N} \tag{3.5}$$

$$\sum_{j:(i,j)\in\mathcal{A}} M_{ij} - \sum_{j:(j,i)\in\mathcal{A}} M_{ji} + mogused_i \left(\sum_{j:(i,j)\in\mathcal{A}} A_{ij} + \sum_{j:(j,i)\in\mathcal{A}} A_{ji} \right) \leq startmog_i \qquad \forall i \in \mathcal{N} \tag{3.6}$$

$$\sum_{i \in \mathcal{N}} Y_i \leq maxattacks \tag{3.7}$$

$$X_{ij}, A_{ij}, M_{ij} \geq 0 \qquad \forall (i,j) \in \mathcal{A} \tag{3.8}$$

$$Y_i \in \{0,1\} \qquad \forall i \in \mathcal{N} \tag{3.9}$$

- The opposing objectives of the attacker and defender are represented in a single objective function, Expression (3.1), in which the defender wants to maximize and the attacker wants to minimize cargo flow. X_{ts} represents an artificial arc drawn from the demand airfield(s) t to the supply airfield(s) s and represents the total flow of cargo through the network. The remaining components of the equation are a penalty assigned to attacked flight legs in the network. For any $q_i > 0$, the corresponding airfield i is susceptible to attack by the adversary.
- The constraint (3.2) is conservation of flow that places a constraint for X_{ts} Every maximum flow problem is structured with a form of this formula.
- The constraint (3.3) limits the amount of cargo flow through a flight leg by the cargo capacity of the number of aircraft assigned to flight leg (i, j) in the connected network

of airfields. It also limits the capacity of the amount of cargo flow through a flight leg by the overall supply of cargo that is desired to flow from the supply airfield(s) s through the network to the demand airfield(s) t.

- The constraint (3.4) limits the amount of WMOG that can be moved between airfields $i \in N$ and $j \in N$ within the network. The movement is captured as flow along a flight leg $(i, j) \in A$.
- The constraint (3.5) ensures the movement of WMOG into an airfield i, along with the starting WMOG already staged at that airfield, does not exceed the maximum amount of WMOG allowed at airfield i.
- The constraint (3.6) ensures that the number of aircraft assigned to flight legs $(i, j) \in A$ and the movement of WMOG does not exceed the capabilities of the WMOG located at airfield i.
- The constraint (3.7) limits the number of attacks an adversary can make on the network of airfields.
- The constraint (3.8) ensures the model outputs only positive values for the flow of cargo, aircraft, and WMOG through the network.
- The constraint (3.9) represents attack on the network of airfields as a binary variable. This variable will either "turn on" or "turn off" the penalty of flow given an attack.

In the next section, we describe a decomposition-based method for solving ADAPT.

3.2 Decomposition Algorithm

We develop a decomposition algorithm to solve ADAPT by separating the model into an operator (AMC/defender perspective) sub-problem and a relaxed master problem (adversary/attacker perspective). It is initiated by applying an attack (represented as an attack vector) composed of no attacks on the operator sub-problem. Given this attack, the sub-problem computes a flow that maximizes the amount of cargo that can be moved through the network. This generates an output for flow, WMOG movement, and aircraft allocation that becomes an input for the relaxed master problem. Given this input of flow, WMOG movement, and aircraft allocation, the relaxed master problem computes the optimal attack vector that minimizes the flow of cargo through the airlift network. This attack vector then becomes an updated input for the operator-sub problem. The algorithm will continue to create new attack vectors for the attacker and flow, WMOG movement, and aircraft allocation for the defender until the possible highest and lowest optimal solution is within an optimality gap ε.

Operator Sub-problem: The variables in this chapter that have the ˆ operator can be interpreted as inputs that were generated from solving another problem. The operator's objective is to maximize the flow of cargo through its network of airfields. To compute this optimal solution, $\hat{Y}$ will be calculated from the relaxed master problem. The initial attack vector is set to 0, translated as the attacker attacking none of the airfields. Based on this input, the operator will calculate the maximum amount of cargo flow through its network of airfields.

$$
\begin{aligned}
\underset{X,A,M}{\text{maximize}} \quad & X_{ts} - \sum_{i \in \mathcal{N}} q_i \hat{Y}_i \left[\sum_{j:(i,j) \in \mathcal{A}} X_{ij} + \sum_{j:(j,i) \in \mathcal{A}} X_{ji} \right] \\
\text{subject to} \quad & \sum_{j:(i,j) \in \mathcal{A}} X_{ij} - \sum_{j:(j,i) \in \mathcal{A}} X_{ji} = \begin{cases} X_{ts}, & \text{if } \ i = s \\ 0, & \text{if } \ i \notin \mathcal{N} \setminus \{s,t\} \\ -X_{ts} & \text{if } \ i = t \end{cases} \\
& X_{ij} \le \begin{cases} cargocap \cdot A_{ij} & \text{if } \ (i,j) \in \mathcal{A} \\ supply & \text{if } \ (i,j) = (t,s) \end{cases} \\
& \sum_{(i,j) \in \mathcal{A}} M_{ij} \le maxmogmoved \\
& - \sum_{j:(i,j) \in \mathcal{A}} M_{ij} + \sum_{j:(j,i) \in \mathcal{A}} M_{ji} \le maxmog_i - startmog_i \qquad \forall i \in \mathcal{N} \\
& \sum_{j:(i,j) \in \mathcal{A}} M_{ij} - \sum_{j:(j,i) \in \mathcal{A}} M_{ji} + \\
& \quad mogused_i \left(\sum_{j:(i,j) \in \mathcal{A}} A_{ij} + \sum_{j:(j,i) \in \mathcal{A}} A_{ji} \right) \le startmog_i \qquad \forall i \in \mathcal{N} \\
& X_{ij}, A_{ij}, M_{ij} \ge 0 \qquad \forall (i,j) \in \mathcal{A}
\end{aligned}
$$

Relaxed Master Problem: The relaxed master problem is solved after the Operator Sub-Problem is solved. The outputs from the Operator Sub-Problem are labeled $\hat{X}, \hat{A}, \hat{M}$. The variable K represents the number of iterations that are completed prior to outputting an optimal solution. As the algorithm iterates through various solutions, it appends constraints to the master problem.

$$
\begin{aligned}
\underset{Z,Y}{\text{minimize}} \quad & Z \\
\text{subject to} \quad & Z \geq \hat{X}_{ts} - \sum_{i \in \mathcal{N}} q_i Y_i \left[\sum_{j:(i,j) \in \mathcal{A}} \hat{X}_{ij} + \sum_{j:(j,i) \in \mathcal{A}} \hat{X}_{ji} \right], \qquad k = 1, \ldots, K \\
& \sum_{(i,j) \in \mathcal{A}} Y_{ij} \leq maxattacks \\
& Y_{ij} \in \{0, 1\} \qquad \forall (i,j) \in \mathcal{A}
\end{aligned}
$$

Decomposition Algorithm: Given the operator and attacker problem, the decomposition algorithm for solving ADAPT is:

1. $LB = -\infty; UB = \infty; K = 1$
2. $\hat{Y} = 0 \forall \ i \in N$
3. While UB - $LB > \varepsilon LB$ (We use $\epsilon = 0.01$.)
4. Solve OPERATOR SUBPROBLEM using $\hat{Y}$ to get:
   $\hat{X}^K = X^*, Q^K = X^*_{t,s} - \sum_{(i,j) \in A}$
5. If $UB > Q^K : UB = Q^K, \hat{Y}^{BEST} = \hat{Y}$
6. Solve ATTACKER RELAXED MASTER using $\hat{X}^1, \hat{X}^2, \ldots \hat{X}^K$ to get:
   $\hat{Y} = Y^*, Z^K = Z^*$
7. If $LB < Z^K : LB = Z^K$
8. $K = K + 1$
9. End While
10. Return $\hat{Y}^{BEST}$ as an ε-optimal solution to the attacker problem

CHAPTER 4:
Analysis

In this chapter, we apply ADAPT to two notional airlift network planning scenarios. The first scenario is a small one meant to illustrate and verify the operation of ADAPT, where the network and the full set of required data can be shown easily. The second scenario is a larger one that involves the potential movement of cargo from the continental United States to Taiwan through a subset of the airfields in the Indo-Pacific area of responsibility.

4.1 Initial Illustrative Scenario

The structure of the network in the first scenario is shown in Figure 4.1. Cargo is supplied from airfield A to meet a demand at airfield E. Airfields B, C, and D are the airfields that are susceptible to an attacker's attacks. The initial WMOG allocation of this network is displayed above each airfield (depicted as a node), with 29 WMOG initially allocated throughout this network. The operator's objective is to move 3,500 cargo-tons of cargo from airfield A to airfield E.

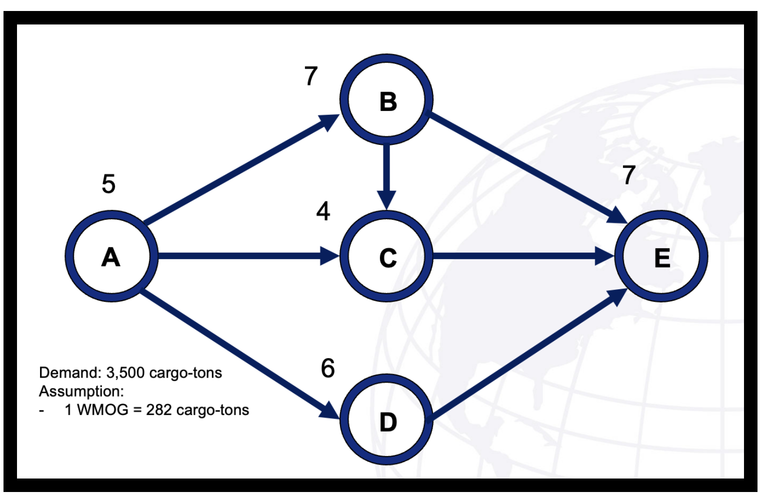

Figure 4.1. Airlift Network

The first step in the decomposition algorithm is to select an initial attack. We explored the impact of one attack on this preliminary network, but there was no solution that would reduce the operator's ability to move 3,500 cargo-tons of cargo from airfield A to E. This illustrates that the current state of the airlift network is resilient against a single attack.

For this scenario, the initial attack is on airfields B and C, shown in Figure 4.2 (highlighted in yellow). In response to this first attack, the decomposition algorithm solves the operator subproblem to determine how much flow the network can support. It turns out that this first attack reduces the operator's ability to move cargo from airfield A to E to 72.5% of the original cargo-tons desired.

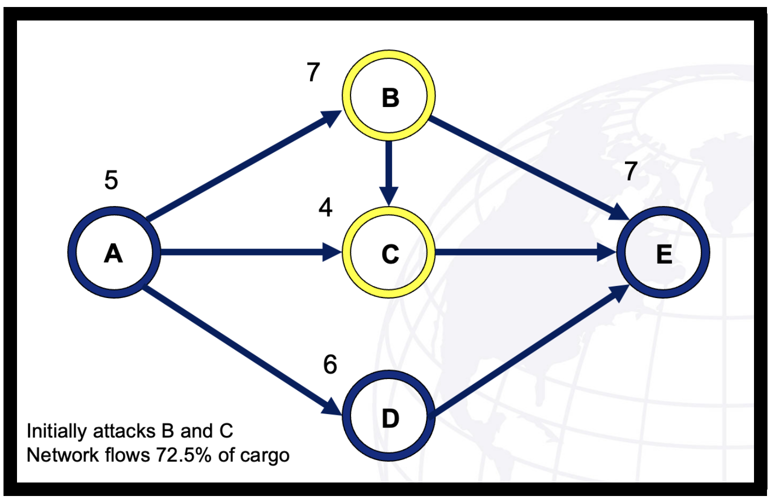

Figure 4.2. Initial Attack

The decomposition algorithm then solves the attacker relaxed master problem to get an updated attack. For this scenario, the updated attack was determined to be airfields B and D. This is shown in Figure 4.3. Solving the operator subproblem reveals that this attack reduces the Operator's ability to move cargo from airfield A to E to 60% of the original cargo-tons desired.

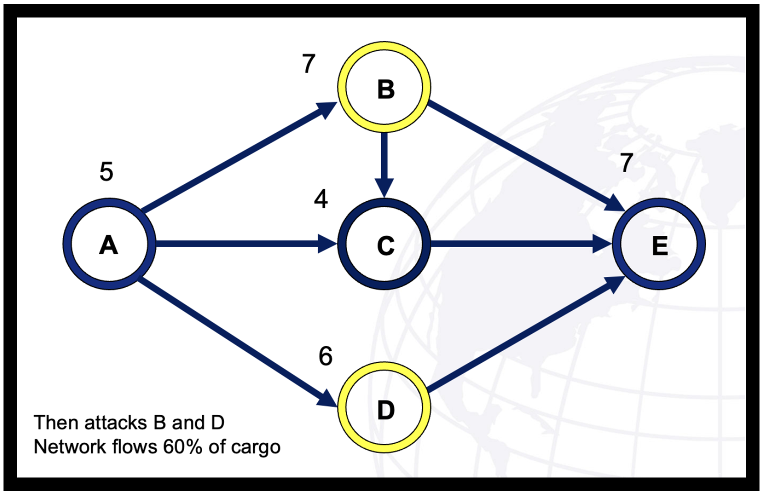

Figure 4.3. Second Attack

The next attack that is generated is shown in Figure 4.4. This attack consists of attacking airfields C and D, which are highlighted in yellow in the figure. This attack reduces the Operator's ability to move cargo from airfield A to node E to 80% of the original cargo-tons desired.

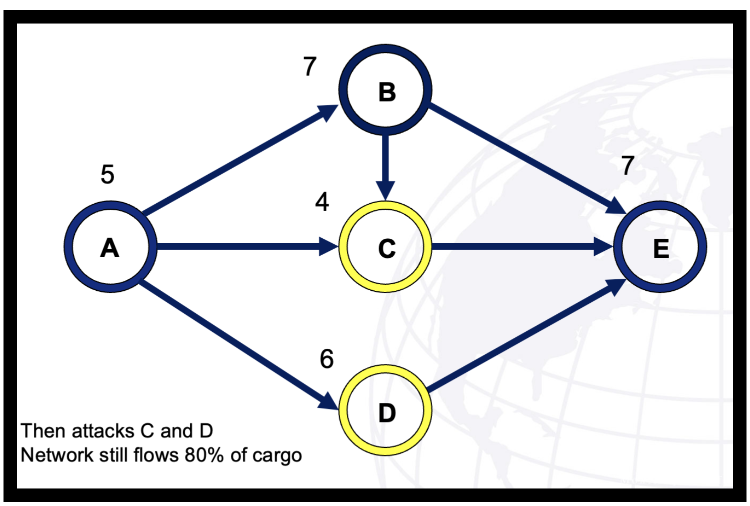

Figure 4.4. Third Attack

The final attack generated by the decomposition algorithm is shown in Figure 4.5. This attack consists of attacking airfields B and D, and reduces the operator's ability to move cargo from airfield A to node E to 60% of the original cargo-tons desired. The operator's optimal response to this attack is to move two WMOG to airfield C by moving one WMOG each from airfield A and B. To move this cargo, there should be 24 aircraft assigned to arc A-C and 24 aircraft to arc D-E.

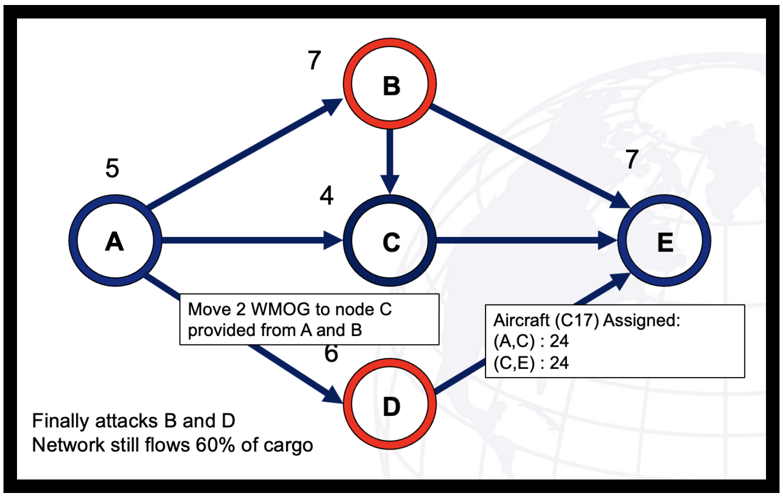

Figure 4.5. Final Attack

4.2 Indo-Pacific Scenario

Next, we apply ADAPT to a larger scenario that is of potential interest to AMC. The inputs for ADAPT containing information about the airfields are provided in Table 4.1, and are depicted in Figure 4.6. The yellow nodes represent 24 airfields across AMC's network of airfields and have 55 WMOG allocated throughout these airfields. The inputs for the flight legs are given in A.1. AMC's objective in this scenario is to deliver 2000 cargo tons of cargo from CONUS (shown as a launching green aircraft) to Taiwan (shown as a landing green aircraft). The red curve represents the range of a DF-26, which can target any airfield within its range. If an airfield is attacked by the DF-26, it will remove the airlift capabilities at the airfield and eliminate cargo flow through the airfield.

Table 4.1. Indo-Pacific Scenario: Airfield Inputs

i	ICAO	AirfieldName	startmog	mogused	maxmog	q
0	CONUS	CONUS	7	0.28	8	0
1	PGUA	Andersen Air Force Base, Guam	4	0.28	8	1
2	NZAA	Auckland International Airport	0	0.28	8	0
3	WBSB	Brunei International Airport	0	0.28	8	1
4	PHNL	Daniel K Inouye International Airport, Hawaii	2.5	0.28	8	0
5	VTBD	Don Mueang International Airport	2	0.28	8	1
6	PAED	Elmendorf Air Force Base, Alaska	2.5	0.28	8	0
7	WAAA	Hasanuddin International Airport	1	0.28	8	1
8	AGGH	Honiara International Airport	1	0.28	8	0
9	RODN	Kadena Air Base, Japan	4	0.28	8	1
10	WMKK	Kuala Lumpur International Airport	1	0.28	8	1
11	WADD	Ngurah Rai (Bali) International Airport	1	0.28	8	1
12	RPLL	Ninoy Aquino International Airport	3	0.28	8	1
13	VVNB	Noi Bai International Airport	2	0.28	8	1
14	NWWM	NoumÃ©a Magenta Airport	1	0.28	8	1
15	RKSO	Osan Air Base, South Korea	4	0.28	8	1
16	YPPH	Perth International Airport	2	0.28	8	0
17	NCRG	Rarotonga International Airport	1	0.28	8	1
18	WSSS	Singapore Changi Airport	2	0.28	8	1
19	WIII	Soekarno-Hatta International Airport	1	0.28	8	1
20	YSSY	Sydney Kingsford Smith International Airport	1	0.28	8	0
21	VVTS	Tan Son Nhat International Airport	1	0.28	8	1
22	RJTY	Yokota Air Base	4	0.28	8	1
23	TAIWAN	TAIWAN	7	0.28	8	0

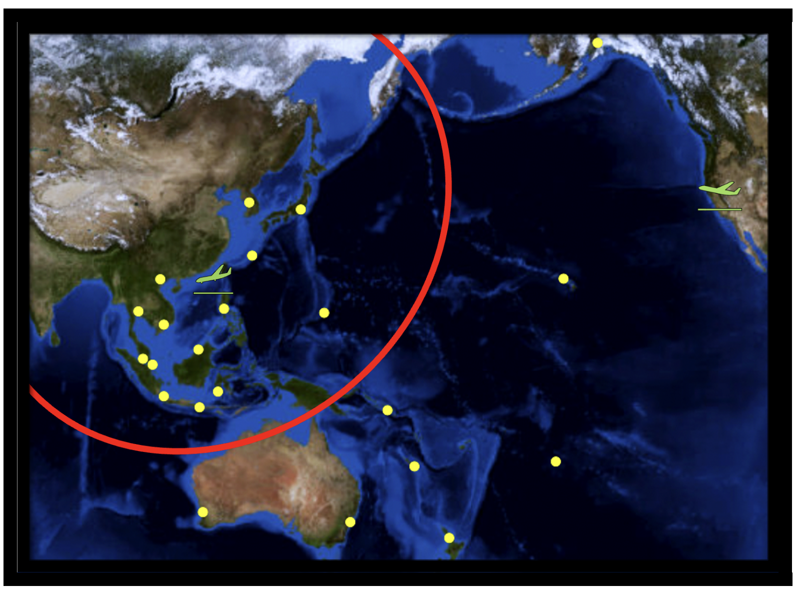

Figure 4.6. Indo-Pacific Scenario

The decomposition algorithm was used to compute the worst-case attacks on this network for varying attack budgets. The worst-case attack when three airfields can be targeted simultaneously is shown in Figure 4.7. Here, the attacker targets Kadena AFB, Okinawa, Japan, Yokosuka AFB, Japan, and Osan AFB, South Korea. This attack would result in AMC only being able to move 96% of cargo through this airlift network.

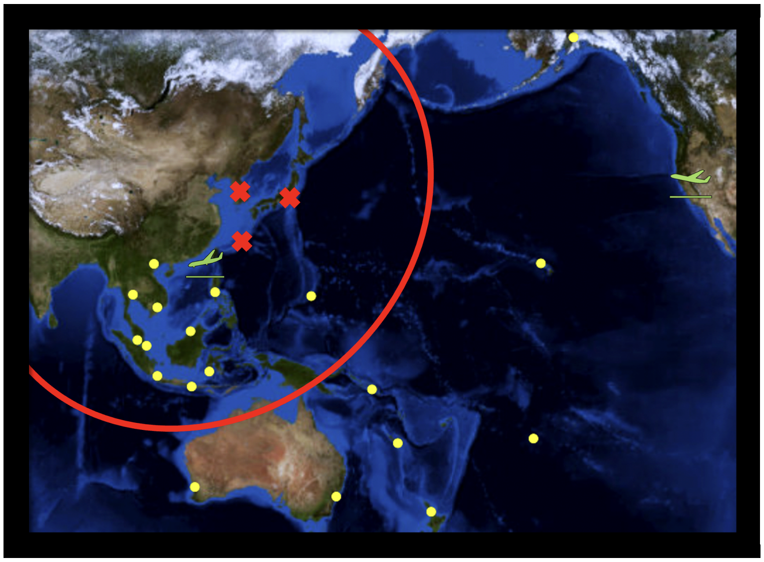

Figure 4.7. Worst-Case Set of Three Airfields to Attack

In addition to identifying which airfields are most valuable for an adversary to attack, ADAPT also outputs the best flow of cargo, aircraft flow, and WMOG to move between airfields in response to the worst-case attack. Table 4.2 shows the flow of cargo through the attacked network. Table 4.3 shows where aircraft will have to flow between airfields. Table 4.4 shows how AMC should adjust its network to maximize the flow of cargo through its airfields based on three attacks.

Table 4.2. Indo-Pacific Scenario: Cargo Flow with Three Attacks

i	j	CargoFlow
PGUA	TAIWAN	2.2
PHNL	TAIWAN	1.5
WMKK	TAIWAN	0.5
RPLL	TAIWAN	2.6
WSSS	VVTS	0.5
YSSY	WMKK	0.5
VVTS	TAIWAN	0.5
CONUS	PGUA	2.2
CONUS	PHNL	1.5
CONUS	RPLL	2.6
CONUS	WSSS	0.5
CONUS	YSSY	0.5

Table 4.3. Indo-Pacific Scenario: Aircraft Placement with Three Attacks

i	j	AircraftPlacement
PGUA	TAIWAN	7.1
PHNL	TAIWAN	4.9
WMKK	TAIWAN	1.8
RPLL	TAIWAN	8.5
WSSS	VVTS	1.8
YSSY	WMKK	1.8
VVTS	TAIWAN	1.8
CONUS	PGUA	7.1
CONUS	PHNL	4.9
CONUS	RPLL	8.5
CONUS	WSSS	1.8
CONUS	YSSY	1.8

Table 4.4. Indo-Pacific Scenario: WMOG Movement with Three Attacks

i	j	WMOG_Movement
RKSO	RPLL	0.8
WSSS	RPLL	1
CONUS	PHNL	0.2

The worst-case attack when four airfields can be simultaneously targeted is shown in Figure 4.8. This attack consists of targeting Kadena AFB, Okinawa, Japan, Yokosuka AFB, Japan, Osan AFB, South Korea and Anderson AFB, Guam. This attack would result in AMC being able to move only 68% of cargo through its network of airfields, compared to when all airfields are operational.

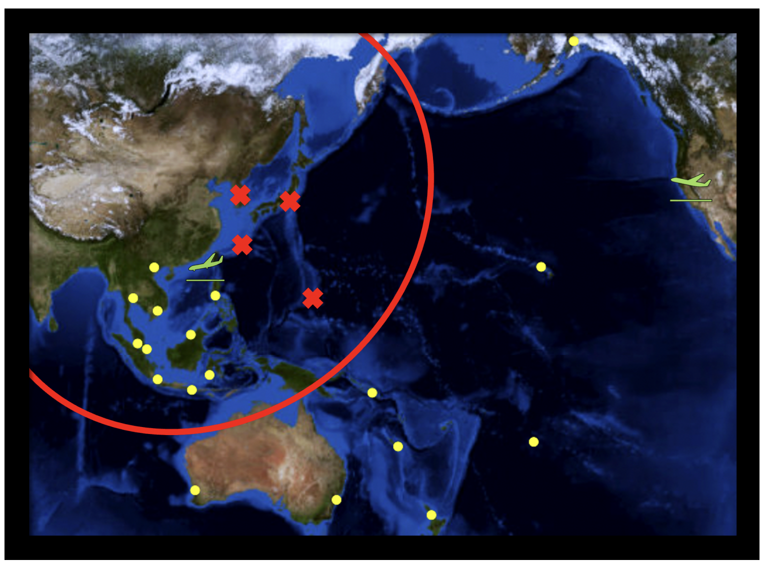

Figure 4.8. Worst-Case Set of Four Airfields to Attack

Table 4.5 shows the flow of cargo through the attacked network. Table 4.6 shows where aircraft will have to flow between airfields. Table 4.7 shows how AMC should adjust its network to maximize the flow of cargo through its airfields based on four attacks.

Table 4.5. Indo-Pacific Scenario: Cargo Flow with Four Attacks

i	j	CargoFlow
PHNL	TAIWAN	2.4
WMKK	TAIWAN	0.5
RPLL	TAIWAN	1.6
WSSS	VVTS	0.5
YSSY	WMKK	0.5
VVTS	TAIWAN	0.5
CONUS	PHNL	2.4
CONUS	RPLL	1.6
CONUS	WSSS	0.5
CONUS	YSSY	0.5

Table 4.6. Indo-Pacific Scenario: Aircraft Placement with Four Attacks

i	j	AircraftPlacement
PHNL	TAIWAN	8
WMKK	TAIWAN	1.8
RPLL	TAIWAN	5.4
WSSS	VVTS	1.8
YSSY	WMKK	1.8
VVTS	TAIWAN	1.8
CONUS	PHNL	8
CONUS	RPLL	5.4
CONUS	WSSS	1.8
CONUS	YSSY	1.8

Table 4.7. Indo-Pacific Scenario: Cargo Flow with Four Attacks

i	j	WMOG_Movement
CONUS	PHNL	2

Figure 4.9 shows the impact of the number of attacks on the amount of cargo that can be moved through the airlift network. The current allocation of airfields is capable of moving 100% of cargo for up to two attacks and decreases as the number of attacks increases. The

decrease is sharp from three to four attacks, but levels off at around 30% beyond eight attacks. Appendix A contains the outputs of ADAPT for up to 10 attacks.

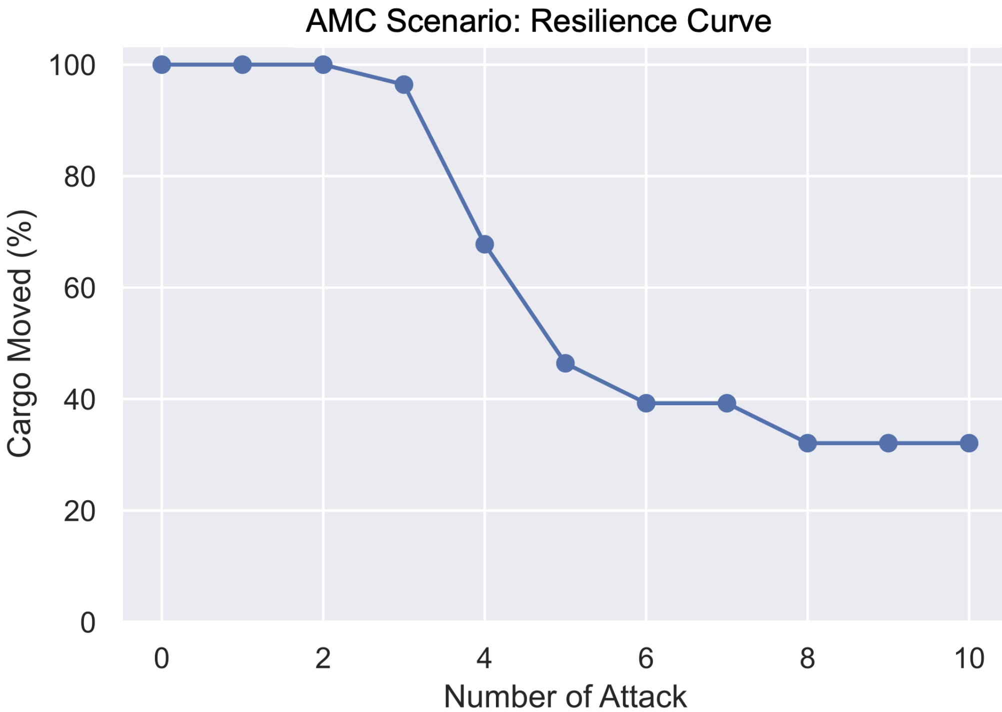

Figure 4.9. Indo-Pacific Scenario: Resilience Curve

CHAPTER 5: Conclusion

This chapter provides final conclusions, recommendations for using the ADAPT model, recommendations for how AMC planners can use the results, and future work that can build on this thesis.

5.1 Conclusions

As AMC develops decision support tools, it must consider the adversary's actions when planning its airlift networks. ADAPT aids AMC planners by detecting vulnerabilities in their network that can be exploited by adversaries. Additionally, ADAPT lays the foundation for incorporating the impact of an attack to airlift plans and infuses contested environments into AMC planner conversations. Identifying which airfields are most valuable for an attacker to attack and having an idea of the overall impact of the attack will assist planners in developing alternative airlift networks to accomplish mission objectives.

5.2 Recommendations

ADAPT provides AMC planners and decision makers with a decision aid that detects airlift network vulnerabilities and prescribes WMOG adjustments and aircraft placement to maximize cargo throughput. The model can be adjusted to assess various threats, such as missiles or cyber threats, that AMC planners may encounter while designing and evaluating their airlift networks.

To leverage ADAPT's capabilities, AMC planners should have a general idea on the threats present in their airlift network, and discuss the impact of that threat. Based on their threat assessment, AMC planners can adjust the coefficient q, which models the impact of an attack at an airfield. The insights gained from ADAPT will provoke discussions that encompass threats in airlift networks, which will aid planners in meeting mission requirements in a contested environment.

5.3 Future Work

This thesis lays the foundation for building models that take an adversary's actions into account when planning an airlift network. Future work that builds on ADAPT should include the impact of an adversary's attack over a period of time. One approach is to have an adversary's attack impact the the flow of cargo over the course of a week, then have the operator adjust its network of WMOG to maximize flow before having the adversary initiate another attack. Another interesting case to explore is incorporating the movement of passengers and its impact on how an adversary would attack the network.

After building a model that identifies the vulnerabilities of the network of airfields, the next research would involve aiding decision-makers in the best response to an attack. Areas to explore would be to reinforce an airfield that is most valuable to attack or adding additional airfields to the network.

For modeling contested logistics, there are various other tools that can aid decision makers that warrant exploration. Modeling contested logistics as a Markov Decision Process (MDP) would incorporate transition probabilities from one state to another state, given a rational decision maker's options. This model would provide insight on the optimal policy (or decision) given the current contested environment. Currently, solving an MDP that models contested logistics is computationally intractable or would require simplifying the model to a point where it begins to be of less use to the decision-maker. As technology develops and new algorithms are discovered, re-visiting modeling contested logistics as an MDP may provide valuable insights.

Another game theoretic approach that could prove useful to model contested logistics is in the form of a Blotto Game. According to Behnezhad et al. (2022), Blotto games are a simultaneous, zero-sum game in which two players allocate resources across battlefields. The winner of each battlefield is determined by which player has more resources allocated to a battlefield and the winner of the game is determined by the player who wins the most battlefields. Behnezhad et al. (2022) developed a technique that makes the solution computationally tractable. In the appropriate contested logistics context, a Blotto game can provide a decision-maker with an optimal strategy for resource allocation and also provide the decision-maker with the optimal strategy for their adversary.

APPENDIX: Tables for Flight Legs and Attack Allocations

This appendix contains details on the flight legs used for the Indo-Pacific scenario described in Chapter 4 and outputs of ADAPT for up to 10 maximum attack allocations for the attacker.

Table A.1. Indo-Pacific Scenario: Flight Leg Inputs

i	ICAO	Airfield	j	Airfield
1	PGUA	Andersen Air Force Base, Guam	9	Kadena Air Base, Japan
1	PGUA	Andersen Air Force Base, Guam	12	Ninoy Aquino International Airport
1	PGUA	Andersen Air Force Base, Guam	22	Yokota Air Base
1	PGUA	Andersen Air Force Base, Guam	15	Osan Air Base, South Korea
1	PGUA	Andersen Air Force Base, Guam	23	TAIWAN
2	NZAA	Auckland International Airport	7	Hasanuddin International Airport
2	NZAA	Auckland International Airport	3	Brunei International Airport
2	NZAA	Auckland International Airport	11	Ngurah Rai (Bali) International Airport
2	NZAA	Auckland International Airport	19	Soekarno-Hatta International Airport
2	NZAA	Auckland International Airport	10	Kuala Lumpur International Airport
2	NZAA	Auckland International Airport	18	Singapore Changi Airport
3	WBSB	Brunei International Airport	9	Kadena Air Base, Japan
3	WBSB	Brunei International Airport	12	Ninoy Aquino International Airport
3	WBSB	Brunei International Airport	21	Tan Son Nhat International Airport
4	PHNL	Daniel K Inouye International Airport, Hawaii	16	Perth International Airport
4	PHNL	Daniel K Inouye International Airport, Hawaii	9	Kadena Air Base, Japan
4	PHNL	Daniel K Inouye International Airport, Hawaii	12	Ninoy Aquino International Airport
4	PHNL	Daniel K Inouye International Airport, Hawaii	22	Yokota Air Base
4	PHNL	Daniel K Inouye International Airport, Hawaii	15	Osan Air Base, South Korea
4	PHNL	Daniel K Inouye International Airport, Hawaii	1	Andersen Air Force Base, Guam
4	PHNL	Daniel K Inouye International Airport, Hawaii	17	Rarotonga International Airport
4	PHNL	Daniel K Inouye International Airport, Hawaii	2	Auckland International Airport
4	PHNL	Daniel K Inouye International Airport, Hawaii	8	Honiara International Airport
4	PHNL	Daniel K Inouye International Airport, Hawaii	20	Sydney Kingsford Smith International Airport
4	PHNL	Daniel K Inouye International Airport, Hawaii	14	NoumÃ©a Magenta Airport
4	PHNL	Daniel K Inouye International Airport, Hawaii	23	TAIWAN
5	VTBD	Don Mueang International Airport	13	Noi Bai International Airport
5	VTBD	Don Mueang International Airport	23	TAIWAN
6	PAED	Elmendorf Air Force Base, Alaska	4	Daniel K Inouye International Airport, Hawaii
6	PAED	Elmendorf Air Force Base, Alaska	9	Kadena Air Base, Japan
6	PAED	Elmendorf Air Force Base, Alaska	12	Ninoy Aquino International Airport
6	PAED	Elmendorf Air Force Base, Alaska	22	Yokota Air Base
6	PAED	Elmendorf Air Force Base, Alaska	15	Osan Air Base, South Korea
6	PAED	Elmendorf Air Force Base, Alaska	1	Andersen Air Force Base, Guam
7	WAAA	Hasanuddin International Airport	9	Kadena Air Base, Japan
7	WAAA	Hasanuddin International Airport	12	Ninoy Aquino International Airport
7	WAAA	Hasanuddin International Airport	21	Tan Son Nhat International Airport
8	AGGH	Honiara International Airport	22	Yokota Air Base
8	AGGH	Honiara International Airport	15	Osan Air Base, South Korea
8	AGGH	Honiara International Airport	12	Ninoy Aquino International Airport
8	AGGH	Honiara International Airport	21	Tan Son Nhat International Airport
9	RODN	Kadena Air Base, Japan	22	Yokota Air Base
9	RODN	Kadena Air Base, Japan	15	Osan Air Base, South Korea
9	RODN	Kadena Air Base, Japan	12	Ninoy Aquino International Airport
9	RODN	Kadena Air Base, Japan	13	Noi Bai International Airport
9	RODN	Kadena Air Base, Japan	23	TAIWAN
10	WMKK	Kuala Lumpur International Airport	9	Kadena Air Base, Japan
10	WMKK	Kuala Lumpur International Airport	12	Ninoy Aquino International Airport
10	WMKK	Kuala Lumpur International Airport	21	Tan Son Nhat International Airport
10	WMKK	Kuala Lumpur International Airport	23	TAIWAN

Table A.2. Indo-Pacific Scenario: Flight Leg Inputs Continued (1/2)

i	ICAO	Airfield	j	Airfield
11	WADD	Ngurah Rai (Bali) International Airport	9	Kadena Air Base, Japan
11	WADD	Ngurah Rai (Bali) International Airport	12	Ninoy Aquino International Airport
11	WADD	Ngurah Rai (Bali) International Airport	21	Tan Son Nhat International Airport
11	WADD	Ngurah Rai (Bali) International Airport	23	TAIWAN
12	RPLL	Ninoy Aquino International Airport	15	Osan Air Base, South Korea
12	RPLL	Ninoy Aquino International Airport	22	Yokota Air Base
12	RPLL	Ninoy Aquino International Airport	13	Noi Bai International Airport
12	RPLL	Ninoy Aquino International Airport	5	Don Mueang International Airport
12	RPLL	Ninoy Aquino International Airport	21	Tan Son Nhat International Airport
12	RPLL	Ninoy Aquino International Airport	23	TAIWAN
13	VVNB	Noi Bai International Airport	15	Osan Air Base, South Korea
13	VVNB	Noi Bai International Airport	22	Yokota Air Base
13	VVNB	Noi Bai International Airport	23	TAIWAN
14	NWWM	NoumÃ©a Magenta Airport	7	Hasanuddin International Airport
14	NWWM	NoumÃ©a Magenta Airport	3	Brunei International Airport
14	NWWM	NoumÃ©a Magenta Airport	11	Ngurah Rai (Bali) International Airport
14	NWWM	NoumÃ©a Magenta Airport	19	Soekarno-Hatta International Airport
14	NWWM	NoumÃ©a Magenta Airport	10	Kuala Lumpur International Airport
14	NWWM	NoumÃ©a Magenta Airport	18	Singapore Changi Airport
15	RKSO	Osan Air Base, South Korea	9	Kadena Air Base, Japan
15	RKSO	Osan Air Base, South Korea	12	Ninoy Aquino International Airport
15	RKSO	Osan Air Base, South Korea	13	Noi Bai International Airport
15	RKSO	Osan Air Base, South Korea	21	Tan Son Nhat International Airport
15	RKSO	Osan Air Base, South Korea	23	TAIWAN
16	YPPH	Perth International Airport	7	Hasanuddin International Airport
16	YPPH	Perth International Airport	3	Brunei International Airport
16	YPPH	Perth International Airport	11	Ngurah Rai (Bali) International Airport
16	YPPH	Perth International Airport	19	Soekarno-Hatta International Airport
16	YPPH	Perth International Airport	10	Kuala Lumpur International Airport
16	YPPH	Perth International Airport	18	Singapore Changi Airport
17	NCRG	Rarotonga International Airport	7	Hasanuddin International Airport
17	NCRG	Rarotonga International Airport	3	Brunei International Airport
17	NCRG	Rarotonga International Airport	11	Ngurah Rai (Bali) International Airport
17	NCRG	Rarotonga International Airport	19	Soekarno-Hatta International Airport
17	NCRG	Rarotonga International Airport	10	Kuala Lumpur International Airport
17	NCRG	Rarotonga International Airport	18	Singapore Changi Airport
18	WSSS	Singapore Changi Airport	9	Kadena Air Base, Japan
18	WSSS	Singapore Changi Airport	12	Ninoy Aquino International Airport
18	WSSS	Singapore Changi Airport	21	Tan Son Nhat International Airport
19	WIII	Soekarno-Hatta International Airport	9	Kadena Air Base, Japan
19	WIII	Soekarno-Hatta International Airport	12	Ninoy Aquino International Airport
19	WIII	Soekarno-Hatta International Airport	21	Tan Son Nhat International Airport

Table A.3. Indo-Pacific Scenario: Flight Leg Inputs Continued (2/2)

i	ICAO	Airfield	j	Airfield
20	YSSY	Sydney Kingsford Smith International Airport	7	Hasanuddin International Airport
20	YSSY	Sydney Kingsford Smith International Airport	3	Brunei International Airport
20	YSSY	Sydney Kingsford Smith International Airport	11	Ngurah Rai (Bali) International Airport
20	YSSY	Sydney Kingsford Smith International Airport	19	Soekarno-Hatta International Airport
20	YSSY	Sydney Kingsford Smith International Airport	10	Kuala Lumpur International Airport
20	YSSY	Sydney Kingsford Smith International Airport	18	Singapore Changi Airport
21	VVTS	Tan Son Nhat International Airport	9	Kadena Air Base, Japan
21	VVTS	Tan Son Nhat International Airport	12	Ninoy Aquino International Airport
21	VVTS	Tan Son Nhat International Airport	23	TAIWAN
22	RJTY	Yokota Air Base	9	Kadena Air Base, Japan
22	RJTY	Yokota Air Base	12	Ninoy Aquino International Airport
22	RJTY	Yokota Air Base	13	Noi Bai International Airport
22	RJTY	Yokota Air Base	23	TAIWAN
0	CONUS	CONUS	1	Andersen Air Force Base, Guam
0	CONUS	CONUS	4	Daniel K Inouye International Airport, Hawaii
0	CONUS	CONUS	6	Elmendorf Air Force Base, Alaska
0	CONUS	CONUS	9	Kadena Air Base, Japan
0	CONUS	CONUS	12	Ninoy Aquino International Airport
0	CONUS	CONUS	15	Osan Air Base, South Korea
0	CONUS	CONUS	18	Singapore Changi Airport
0	CONUS	CONUS	20	Sydney Kingsford Smith International Airport
0	CONUS	CONUS	22	Yokota Air Base

A.1 Max Attacks = 0

Table A.4. Indo-Pacific Scenario: Cargo Flow Zero Attacks

i	j	CargoFlow
PGUA	TAIWAN	2.2
RODN	TAIWAN	2.2
RPLL	TAIWAN	1.6
RJTY	TAIWAN	1.6
CONUS	PGUA	2.2
CONUS	RODN	2.2
CONUS	RPLL	1.6
CONUS	RJTY	1.6

Table A.5. Indo-Pacific Scenario: Aircraft Placement Zero Attacks

i	j	AircraftPlacement
PGUA	TAIWAN	7.1
RODN	TAIWAN	7.1
RPLL	TAIWAN	5.4
RJTY	TAIWAN	5.4
CONUS	PGUA	7.1
CONUS	RODN	7.1
CONUS	RPLL	5.4
CONUS	RJTY	5.4

Table A.6. Indo-Pacific Scenario: WMOG Shift Zero Attacks

i	j	WMOG_Shift

A.2 Max Attacks = 1

Table A.7. Indo-Pacific Scenario: Cargo Flow One Attack

i	j	CargoFlow
PGUA	TAIWAN	2.2
RODN	TAIWAN	2.2
RPLL	TAIWAN	1.6
RJTY	TAIWAN	1.6
CONUS	PGUA	2.2
CONUS	RODN	2.2
CONUS	RPLL	1.6
CONUS	RJTY	1.6

Table A.8. Indo-Pacific Scenario: Aircraft Placement One Attack

i	j	AircraftPlacement
PGUA	TAIWAN	7.1
RODN	TAIWAN	7.1
RPLL	TAIWAN	5.4
RJTY	TAIWAN	5.4
CONUS	PGUA	7.1
CONUS	RODN	7.1
CONUS	RPLL	5.4
CONUS	RJTY	5.4

Table A.9. Indo-Pacific Scenario: WMOG Shift One Attack

i	j	WMOG_Shift

A.3 Max Attacks = 2

Table A.10. Indo-Pacific Scenario: Cargo Flow Two Attacks

i	j	CargoFlow
PGUA	TAIWAN	2.2
RODN	TAIWAN	2.2
RPLL	TAIWAN	1.6
RJTY	TAIWAN	1.6
CONUS	PGUA	2.2
CONUS	RODN	2.2
CONUS	RPLL	1.6
CONUS	RJTY	1.6

Table A.11. Indo-Pacific Scenario: Aircraft Placement Two Attacks

i	j	AircraftPlacement
PGUA	TAIWAN	7.1
RODN	TAIWAN	7.1
RPLL	TAIWAN	5.4
RJTY	TAIWAN	5.4
CONUS	PGUA	7.1
CONUS	RODN	7.1
CONUS	RPLL	5.4
CONUS	RJTY	5.4

Table A.12. Indo-Pacific Scenario: WMOG Shift Two Attacks

i	j	WMOG_Shift

A.4 Max Attacks = 3

Table A.13. Indo-Pacific Scenario: Cargo Flow with Three Attacks

i	j	CargoFlow
PGUA	TAIWAN	2.2
PHNL	TAIWAN	1.5
WMKK	TAIWAN	0.5
RPLL	TAIWAN	2.6
WSSS	VVTS	0.5
YSSY	WMKK	0.5
VVTS	TAIWAN	0.5
CONUS	PGUA	2.2
CONUS	PHNL	1.5
CONUS	RPLL	2.6
CONUS	WSSS	0.5
CONUS	YSSY	0.5

Table A.14. Indo-Pacific Scenario: Aircraft Placement with Three Attacks

i	j	AircraftPlacement
PGUA	TAIWAN	7.1
PHNL	TAIWAN	4.9
WMKK	TAIWAN	1.8
RPLL	TAIWAN	8.5
WSSS	VVTS	1.8
YSSY	WMKK	1.8
VVTS	TAIWAN	1.8
CONUS	PGUA	7.1
CONUS	PHNL	4.9
CONUS	RPLL	8.5
CONUS	WSSS	1.8
CONUS	YSSY	1.8

Table A.15. Indo-Pacific Scenario: WMOG Shift with Three Attacks

i	**j**	**WMOG_Shift**
RKSO	RPLL	0.8
WSSS	RPLL	1
CONUS	PHNL	0.2

A.5 Max Attacks = 4

Table A.16. Indo-Pacific Scenario: Cargo Flow with Four Attacks

i	j	CargoFlow
PHNL	TAIWAN	2.4
WMKK	TAIWAN	0.5
RPLL	TAIWAN	1.6
WSSS	VVTS	0.5
YSSY	WMKK	0.5
VVTS	TAIWAN	0.5
CONUS	PHNL	2.4
CONUS	RPLL	1.6
CONUS	WSSS	0.5
CONUS	YSSY	0.5

Table A.17. Indo-Pacific Scenario: Aircraft Placement with Four Attacks

i	j	AircraftPlacement
PHNL	TAIWAN	8
WMKK	TAIWAN	1.8
RPLL	TAIWAN	5.4
WSSS	VVTS	1.8
YSSY	WMKK	1.8
VVTS	TAIWAN	1.8
CONUS	PHNL	8
CONUS	RPLL	5.4
CONUS	WSSS	1.8
CONUS	YSSY	1.8

Table A.18. Indo-Pacific Scenario: WMOG Shift with Four Attacks

i	j	WMOG_Shift
CONUS	PHNL	2

A.6 Max Attacks = 5

Table A.19. Indo-Pacific Scenario: Cargo Flow Five Attacks

i	**j**	**CargoFlow**
PHNL	TAIWAN	2.4
WADD	TAIWAN	0.5
WSSS	VVTS	0.5
YSSY	WADD	0.5
VVTS	TAIWAN	0.5
CONUS	PHNL	2.4
CONUS	WSSS	0.5
CONUS	YSSY	0.5

Table A.20. Indo-Pacific Scenario: Aircraft Placement Five Attacks

i	**j**	**AircraftPlacement**
PHNL	TAIWAN	8
WADD	TAIWAN	1.8
WSSS	VVTS	1.8
YSSY	WADD	1.8
VVTS	TAIWAN	1.8
CONUS	PHNL	8
CONUS	WSSS	1.8
CONUS	YSSY	1.8

Table A.21. Indo-Pacific Scenario: WMOG Shift Five Attacks

i	j	WMOG_Shift
CONUS	PHNL	2

A.7 Max Attacks = 6

Table A.22. Indo-Pacific Scenario: Cargo Flow Six Attacks

i	j	CargoFlow
PHNL	TAIWAN	2.4
WMKK	TAIWAN	0.5
YSSY	WMKK	0.5
CONUS	PHNL	2.4
CONUS	YSSY	0.5

Table A.23. Indo-Pacific Scenario: Aircraft Placement Six Attacks

i	j	AircraftPlacement
PHNL	TAIWAN	8
WMKK	TAIWAN	1.8
YSSY	WMKK	1.8
CONUS	PHNL	8
CONUS	YSSY	1.8

Table A.24. Indo-Pacific Scenario: WMOG Shift Six Attacks

i	j	WMOG_Shift
CONUS	PHNL	2

A.8 Max Attacks = 7

Table A.25. Indo-Pacific Scenario: Cargo Shift Seven Attacks

i	j	CargoFlow
PHNL	TAIWAN	2.4
WMKK	TAIWAN	0.5
YSSY	WMKK	0.5
CONUS	PHNL	2.4
CONUS	YSSY	0.5

Table A.26. Indo-Pacific Scenario: Aircraft Placement Seven Attacks

i	j	AircraftPlacement
PHNL	TAIWAN	8
WMKK	TAIWAN	1.8
YSSY	WMKK	1.8
CONUS	PHNL	8
CONUS	YSSY	1.8

Table A.27. Indo-Pacific Scenario: WMOG Shift Seven Attacks

i	j	WMOG_Shift
CONUS	PHNL	2

A.9 Max Attacks = 8

Table A.28. Indo-Pacific Scenario: Cargo Flow Eight Attacks

i	j	CargoFlow
PHNL	TAIWAN	2.4
CONUS	PHNL	2.4

Table A.29. Indo-Pacific Scenario: Aircraft Placement Eight Attacks

i	j	AircraftPlacement
PHNL	TAIWAN	8
CONUS	PHNL	8

Table A.30. Indo-Pacific Scenario: WMOG Shift Eight Attacks

i	j	WMOG_Shift
CONUS	PHNL	2

A.10 Max Attacks = 9

Table A.31. Indo-Pacific Scenario: Cargo Flow Nine Attacks

i	j	CargoFlow
PHNL	TAIWAN	2.4
CONUS	PHNL	2.4

Table A.32. Indo-Pacific Scenario: Aircraft Placement Nine Attacks

i	j	AircraftPlacement
PHNL	TAIWAN	8
CONUS	PHNL	8

Table A.33. Indo-Pacific Scenario: WMOG Shift Nine Attacks

i	j	WMOG_Shift
CONUS	PHNL	2

A.11 Max Attacks = 10

Table A.34. Indo-Pacific Scenario: Cargo Flow Ten Attacks

i	j	CargoFlow
PHNL	TAIWAN	2.4
CONUS	PHNL	2.4

Table A.35. Indo-Pacific Scenario: Aircraft Placement Ten Attacks

i	j	AircraftPlacement
PHNL	TAIWAN	8
CONUS	PHNL	8

Table A.36. Indo-Pacific Scenario: WMOG Shift Ten Attacks

i	j	WMOG_Shift
CONUS	PHNL	2

List of References

Air Mobility Command (2023a) Air Mobility Command. https://www.amc.af.mil/About-Us/Fact-Sheets/Display/Article/1517710/air-mobility-command/.

Air Mobility Command (2023b) Air Mobility Command fact sheets. https://www.amc.af.mil/About-Us/Fact-Sheets/.

Alderson D, Brown G, Carlyle WM, Wood K (2011) Solving defender-attacker-defender models for infrastructure defense. *12th INFORMS Computing Society Conference* 28–49.

Behnezhad S, Dehghani S, Derakhshan M, Hajiaghayi M, Seddighin S (2022) Fast and simple solutions of Blotto games. *Operations Research* Articles in Advance:1–11.

Brown G, Carlyle WM, Dell R, Brau J (2013) Optimizing intratheater military airlift in Iraq and Afghanistan. *Military Operations Research* 18(3):35–52.

Cormican K, Morton D, Wood K (1998) Stochastic network interdiction. *Operations Research* 46(2):184–197.

Department of Defense (2022) National Defense Strategy of the United States of America. https://www.defense.gov/News/Releases/Release/Article/3201683/department-of-defense-releases-its-2022-strategic-reviews-national-defense-stra/.

Secretary of the Air Force (2018) *Air Mobility Planning Factors*. https://static.e-publishing.af.mil/production/1/af_a3/publication/afpam10-1403/afpam10-1403.pdf.

Trask T (2022) Runtime Analysis of Bender's Decomposition and Dual ILP Algorithms As Applied to Common Network Interdiction Problems. Master's thesis, Naval Postgraduate School, Monterey, CA, http://hdl.handle.net/10945/70770.

Whitlow J (2022) Rapid Operational Design of Airlift Networks in Contested Environments. Master's thesis, Naval Postgraduate School, Monterey, CA.

THIS PAGE INTENTIONALLY LEFT BLANK

Initial Distribution List

1. Defense Technical Information Center
   Ft. Belvoir, Virginia

2. Dudley Knox Library
   Naval Postgraduate School
   Monterey, California